Available online at www.sciencedirect.com
SCIENCE DIRECT
Journal of Photochemistry and Photobiology A: Chemistry 179 (2006) 20–27
Journal of Photochemistry and Photobiology A:Chemistry
www.elsevier.com/locate/jphotochem

Effect of TiO_2 acidic pre-treatment on the photocatalytic properties for phenol degradation

G. Colón*, J.M. Sánchez-España, M.C. Hidalgo, J.A. Navío

Instituto de Ciencia de Materiales de Sevilla, Centro Mixto Universidad de Sevilla-CSIC, Americo Vespucio s/n, 41092 Sevilla, Spain

Received 10 May 2005; received in revised form 13 June 2005; accepted 4 July 2005
Available online 19 August 2005

Abstract

Photocatalytic oxidation of phenol was performed over acid pre-treated TiO_2 prepared by a sol–gel method. Several oxoacids were used in the acid pre-treatment (nitric, sulfuric and phosphoric acids). Wide structural and surface characterisation of catalysts was carried out in order to establish a correlation between the oxoanion stability during calcination and the further photocatalytic behaviour of TiO_2. Pre-treatment with sulfuric and phosphoric acids clearly stabilises TiO_2 catalyst against sintering, maintaining anatase phase and relatively high surface area values with respect to untreated TiO_2. On the other hand, nitric pre-treatment seems to favour sintering process. Acid treatment leads to an excess of adsorbed protons (Brönsted acid sites) incorporated to the TiO_2 surface. During calcination, the elimination of these hydroxyl groups would be the responsible for the generation of a highly defective material that readily losses the oxygen ions from their surface. Different stability of adsorbed oxoanions would stabilise the anatase crystal phase as well these oxygen vacancies formed during calcination, preventing at the same time the sintering process. The occurrence of oxygen vacancies could favour the appearance of small rutile phase dispersed onto the surface of an anatase matrix performing the photoinduced electronic process. Best photocatalytic behaviour is found for pre-sulfated TiO_2 samples calcined at such high temperature for which sulfates have been eliminated.

Keywords: TiO_2; Acid treatment; Oxygen vacancies; Photocatalysis; Phenol oxidation; Rutile–anatase

1. Introduction

Photocatalytic degradation of organic pollutants are becoming one of the most promising green chemistry technology [1–3]. The improvement and optimisation of TiO_2 as photocatalyst is an important task for technical applications of heterogeneous photocatalysis in the future. In this sense, it is well known that the photocatalytic activity of TiO_2 powder strongly depends on its bulk and surface properties [4]. Two of the most representative polymorphs of TiO_2 (anatase and rutile) have received much interest because of their applications such as photocatalysis. The preparation of TiO_2 based on the hydrolysis and condensation of titanium precursor is one of the most reported preparation methods. Further peptisation, by acid treatment, leads to redispersion of the coagulated colloidal particles formed in the sol–gel process. It is well known that acid peptisation using hydrochloric and nitric acid clearly promotes the formation of rutile phase [5,6]. On the contrary, it has been reported that peptisation produced by sulfuric acid retards the anatase to rutile transformation [7]. Thus it is clear that the anatase to rutile transformation depends on the presence of this acid in the preparation solution.

Recently, it has been reported that sulfuric acid impregnated TiO_2 could have interesting photocatalytic properties in certain reactions [8–10]. The enhancement of acidity of the semiconductor is reported as a feasible way to enhance the photocatalytic activity of TiO_2. These papers concluded that the improved efficiency of the sulfated materials was due to a greater surface area as well as to a larger fraction of anatase phase. However the increase of acid properties cannot be ruled out. Deng et al. also reported the effect of sulfation on the photocatalytic activity of TiO_2 for hexane

* Corresponding author.
E-mail address: gcolon@icmse.csic.es (G. Colón).

1010-6030/$ – see front matter © 2005 Elsevier B.V. All rights reserved.
doi:10.1016/j.jphotochem.2005.07.007

and benzene oxidation [11]. They also concluded that the improved photocatalytic activity of sulfated TiO_2 should be caused by a combining effect of the presence of sulfate on the catalyst surface and the increase in catalyst surface area. Similar conclusion was reported by Gomez et al. [12], which suggested that sulfate anchored on the anatase surface acts as electron trap during the photoactivation process.

In a previous paper we had presented results on the photocatalytic activity of sulfated TiO_2 [13]. Surprisingly, these TiO_2/SO_4^{2-} systems exhibited the best photonic efficiencies after calcination at 700 °C. We tentatively assumed there that hyperacid properties would not be the reason of the enhanced photocatalytic behaviour, as other authors proposed. We stated that the surface superacidity should be lost during calcination at that temperature since most of sulfate groups have already been removed with temperature. Thus, the weight loss of TG analysis suggested that the amount of sulfate present might be negligible after calcination at temperature higher than 650 °C. Consequently, we assumed that at that temperature the sulfate species would not improve the acid properties of the catalyst and, therefore, that the enhancement of the photocatalytic activity should be determined by other reasons. The origin of improved efficiency by sulfate on the photocatalytic efficiency of TiO_2 is actually controversial, especially those hypotheses based on the acid properties of TiO_2.

In the present paper, we compare the effect of different inorganic acids (nitric, sulfuric and phosphoric acids) incorporated by impregnation, on the structural and surface evolution of TiO_2 during calcination. The different thermal stability of each one would be correlated with the structural and surface evolution of impregnated TiO_2 and with its photocatalytic activity for phenol degradation.

2. Experimental

2.1. Catalysts preparation

TiO_2 was prepared by a sol–gel method using titanium tetraisopropoxide (TTIP) as precursor in isopropanol. Hydrolysis of the isopropanol-TTIP solution was achieved by adding certain volume of bidistilled water (TTIP:H_2O = 0.05). The precipitate was then filtered and dried at 120 °C overnight and divided in two portions, being one of this portion the untreated TiO_2. Acidification of the other batch was performed by dispersing the fresh dried powders in the corresponding acid solution (1 M nitric, sulfuric and phosphoric acid solution, 50 ml/g) for 1 h. Then, the suspension was filtered off and the powder dried again at 120 °C overnight. Portions of the acid treated TiO_2 samples (hereafter, TN, TS and TP series) were calcined in air at temperatures between 400 and 800 °C for 2 h. Calcined catalysts will be labelled hereafter by adding a number to the series label that indicates the temperature of calcination (i.e. T7, TS7 or TN7 will mean samples of these series calcined at 700 °C).

2.2. Surface and structural characterisation

BET surface area (S_{BET}) and porosity measurements were carried out by N_2 adsorption at 77 K using a Micromeritics 2000 instrument. Pore volumes were determined using the cumulative adsorption of nitrogen by the BJH method.

Thermal evolution of the samples under dynamic conditions was studied by DTA–TGA (differential thermal and thermogravimetric analysis). These curves were obtained simultaneously in static air with a SII Seiko instrument Exstar 6000; model TG/DTA 6300 at a heating rate of 10 °C/min. Calcined alumina was used as reference material.

X-ray diffraction (XRD) patterns were obtained using a Siemens D-501 diffractometer with Ni filter and graphite monochromator with a Cu Kα X-ray source. Anatase–rutile fractions were calculated by taking into account the relative diffraction peak intensities using the following expression [14]:

$$F_A = \frac{0.79 I_A}{0.79 I_A + I_R}$$

From the line broadening of corresponding X-ray diffraction peaks, crystallite size were calculated according to the Warren and Averbach equation by fitting the peaks using a Voigt function

$$D = \frac{\lambda 180}{\pi \cos\theta L}$$

where L is the line width at medium height, λ the wavelength of the X-ray radiation (0.15406 nm) and θ is the diffracting angle.

UV–vis spectra were recorded in the diffuse reflectance mode (R) and transformed to a magnitude proportional to the extinction coefficient (K) through the Kubelka–Munk function, $F(R_\infty)$. Samples were mixed with $BaSO_4$ that does not absorb in the UV–vis radiation range (white standard). Scan range was 240–800 nm.

2.3. Catalytic runs

Photocatalytic runs (2 h) of oxidation of phenol over TN, TS and TP samples (1 g/l) were performed in a Pyrex immersion well reactor (450 ml) using a medium pressure 400 W Hg lamp supplied by Applied Photophysics as light source. In the oxidation tests, an oxygen flow was employed to produce a homogenous suspension of the catalyst in the solution. Before each experiment, the catalysts were settled in suspension with the reagent mixture for 15 min in the dark for the equilibrium of the system. The evolution of the initial phenol concentration (ca. 50 ppm) was followed through the evolution of its characteristic 270 nm band using filtered aliquot (ca. 2 ml) of the suspension (Millipore Millex 25 0.45 μm membrane filter) taken at different irradiation times.

Table 1
BET surface area (m^2/g) for the different acid treated TiO_2 samples

Calcination temperature (°C)	TiO_2	TN	TS	TP
400	98	105	90	129
500	28	45	88	–
600	17	7	41	82
650	–	–	28	–
700	6	<1	20	32
800	<1	<1	6	11

3. Results

In Table 1 are summarised the surface areas of TiO_2 treated with different acids and calcined at different temperatures. As the calcination temperature increases, BET surface area of TiO_2 decreases progressively, reaching the lowest values at $T > 600\,^{\circ}C$. In general acid treatment of the precursor clearly produces a certain stabilisation of the surface area, more significant depending on the acid used. It is well known the surface stabilisation effects reported for sulfate and phosphate promoted systems upon S_{BET} [13–15]. At the same time, it can be observed that for nitric pre-treatment this stabilisation is not observed at all (Table 1). Initial high surface area observed for this sample calcined at 400 °C drastically decays as calcination temperature increases. Moreover, S_{BET} values are even lower than those observed for unmodified TiO_2 calcined at same temperatures.

Weight losses observed by TG measurements are shown in Fig. 1. These weight losses might be ascribed to dehydration/dehydroxylation processes. In the case of TN and TS samples an additional weight loss occurs corresponding to nitrate or sulfate oxoanions decomposition. The profiles of the DTG curves of different samples calcined at $T < 400\,^{\circ}C$ are quite different (Fig. 1). TiO_2 precursor shows a main peak at ca. 70 °C and smaller ones at 220, 280 and 370 °C on a long tail that vanishes at 600 °C. At the same time, for TN precursor, peaks corresponding to weight losses at $T < 400\,^{\circ}C$ can also be observed, though the intensities of them are quite different from those found for TiO_2. The main peak observed for TiO_2 decreased for TN, while peaks corresponding to weight losses between 100 and 400 °C present higher intensities in TN sample. The diminution in weight loss at $T < 100\,^{\circ}C$ can

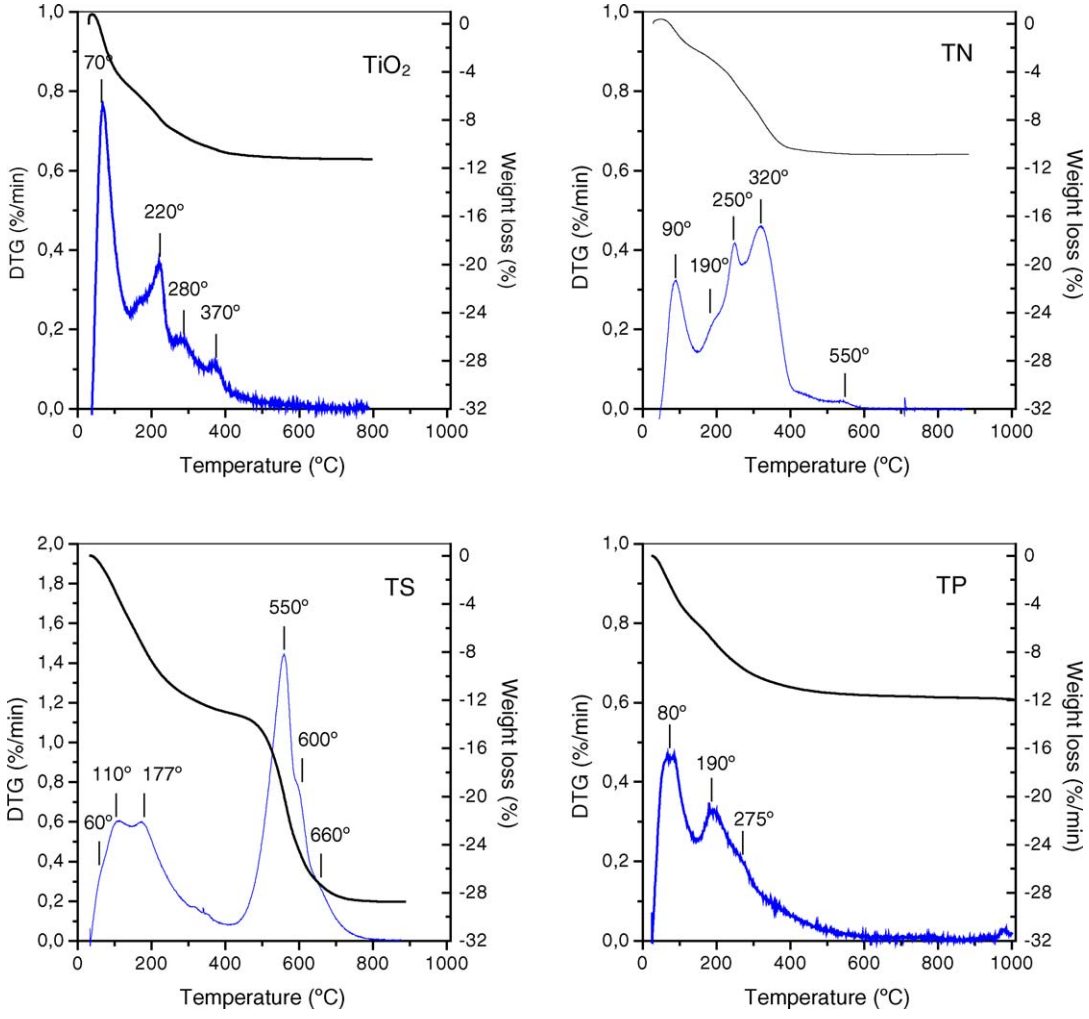

Fig. 1. Thermal analysis (DTG and TG curves) of TiO_2 and the acid pre-treated TiO_2 catalysts.

be explained by the substitution of the surface OH in TiO_2 by the oxoanion during the impregnation process. Additionally the increasing of the weight loss process at temperature between 100 and 400 °C in TN correspond to the elimination of nitrates as well as organic rest from the alkoxide precursor.

For the TS precursor, a small shoulder at ca. 60 °C besides the peak at 110 °C that overlaps with a new intense peak at 177 °C is observed. Once more, the attenuation of the weight loss at $T < 100$ °C of this sample respect to the untreated TiO_2 could be attributed to the OH substitution by sulfates at the surface. At $T > 400$ °C a large DTG peak is found. This weight loss progress in three steps, as it can be inferred from the curve. This three step weight loss is due to the decomposition of surface sulfates, anchored at the surface forming a multilayer. Thus, a first decomposition at 550 °C could correspond to the elimination of the weakest sulfate groups; while at 660 °C would take place the decomposition of the stronger sulfates. Different temperature programmed desorption experiments previously reported [16], showed the loss of water and hydroxyl groups from TiO_2 (Degussa P25) treated with NaOH and HCl solutions. This acid and basic treatment greatly modified the relative amounts of basic and acid surface OH-groups (OH^-/H^+ equilibrium) and thus the efficiency of TiO_2 in the photoadsorption of oxygen under UV-irradiation. Dispersion of our TiO_2-precursor in the 1 M H_2SO_4 or HNO_3 solutions (pH ~1) must also produce an "electrical double layer", according to the Stern model [17]. Thus, our colloidal TiO_2 particles should present an excess of protons at their surface. Therefore, surface might be considered as a diffuse layer with an excess of charge, formed by compensating NO_3^- or SO_4^{2-} ions retained upon filtering. By observing the TG curves it is clear that sulfates are more strongly retained at the surface than nitrates, leading to significantly different total weight losses.

TP system only presents the weight loss corresponding to the elimination of water/hydroxyl groups and the alkoxide rests, with DTG evolution similar to those observed for TiO_2. Thus, as expected, surface phosphates groups should remain adsorbed throughout the calcination.

Therefore, the temperature stability of the adsorbed oxoanions can be stated by observing the evolution of the different acid promoted TiO_2 precursor during calcination. The presence of adsorbed oxoanion has a direct relationship with the stabilisation against sintering process. The stability of the oxoanions can be correlated with the evolution of crystallite size and anatase to rutile transformation. Anatase crystallite size evolution during calcination strongly depends on the nature of the adsorbed oxoanion (Fig. 2). Thus, TiO_2 pretreated with nitric acid (TN) suffers a drastic sintering process compared to TS and TP systems. The behaviour of TN sample during calcination is similar to untreated TiO_2. However, in the case of TN sintering is accompanied with a rapid rutilisation process and rutile phase drastically appears after calcination at 500 °C (Table 2 and Fig. 2). Thus, rutilisation process seems to be accelerated in the case of TN system with respect to TS. Stabilisation of anatase phase clearly depends on the

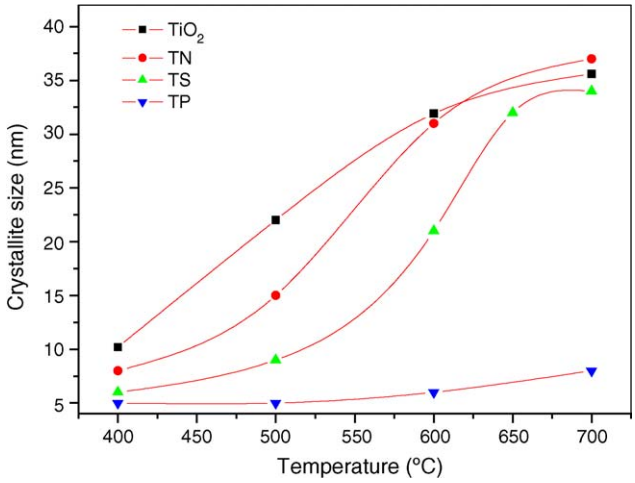

Fig. 2. Evolution of crystallite size of TiO_2 and the acid pre-treated TiO_2 catalysts with the calcination temperature.

stability of the adsorbed oxoanion. Comparing the results from TG/DTG measurements (Fig. 1) with the crystalline phase composition of the samples (Table 2), it can be observed that the rutilisation process only starts to take place when the adsorbed oxoanions decompose. Sulfated TiO_2 (TS) presents stable anatase phase even till relatively high calcination temperature; rutile phase appear just at calcination temperature higher than 650 °C. On the other hand, for TP material, rutile phase is not observed even on calcination at 800 °C. In spite of this, since adsorbed phosphate groups remains at the surface during the whole calcination process, phosphate-like species are formed (Table 2). From XRD pattern of TP calcined at 700 and 800 °C (Fig. 3) it is clear the appearance of titanyl pyrophosphate species $(TiO)_2P_2O_7$ together with anatase. It is reported that the addition of phosphate hinders the surface ionic mobility and, therefore, strongly inhibits the anatase–rutile conversion through a mechanism that implies its chemisorption on TiO_2 as a bidentate ligand [18].

In Fig. 4 we show the UV–vis diffuse reflectance spectra for the different acid pre-treated TiO_2. Inset figures represent the evolution of absorbance in the visible region. It can be observed that as calcination temperature increases, the absorption edge experiments a slight shift towards lower energies for all systems, indicating the appearance of the rutile phase. It is worthy to note that new small absorption band can be found in the visible region. This new band emerges at a certain calcination temperature, depending on the oxoanion.

Table 2
Anatase fraction (%) for the different acid treated TiO_2 samples

Calcination temperature (°C)	TiO_2	TN	TS	TP
400	100	100	100	100
500	100	100	100	100
600	29	14	100	100
650	–	–	100	–
700	6	2	40	100 + $(TiO)_2P_2O_7$
800	0	0	0	100 + $(TiO)_2P_2O_7$

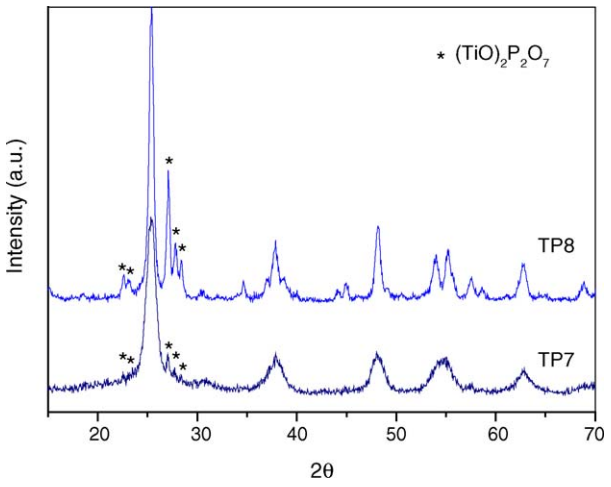

Fig. 3. X-ray diffraction pattern for phosphoric acid pre-treated TiO_2 catalyst calcined at 700 and 800 °C.

Thus, this small visible absorption takes place for TP6, TS7 and TN5, being the intensity of this absorption significantly lower for the TN system.

In a previous paper we reported the existence of a new contribution in the UV–vis spectra of sulfated TiO_2 calcined at temperatures higher than 600 °C [13]. This new band in the visible range was associated to the existence of oxygen vacancies derived from the acidification pre-treatment [16]. Acidification process generates a highly protonated surface that upon calcination would lead to the formation of surface oxygen vacancies. In the presence of surface sulfates these vacancies could be stabilised in a subsurface layer. From results in Fig. 4, it can be inferred that the disappearance of these oxygen vacancies could be directly related with the temperature at which each oxoanion is eliminated from the surface. At the same time the stability of each oxoanion clearly determine the rutilisation process. In the case of nitric acid pre-treated TiO_2, vacancies formation would occur at the same time as nitrate decomposition. Elimination of nitrates could avoid the stabilisation of the vacancies in a sub-surface

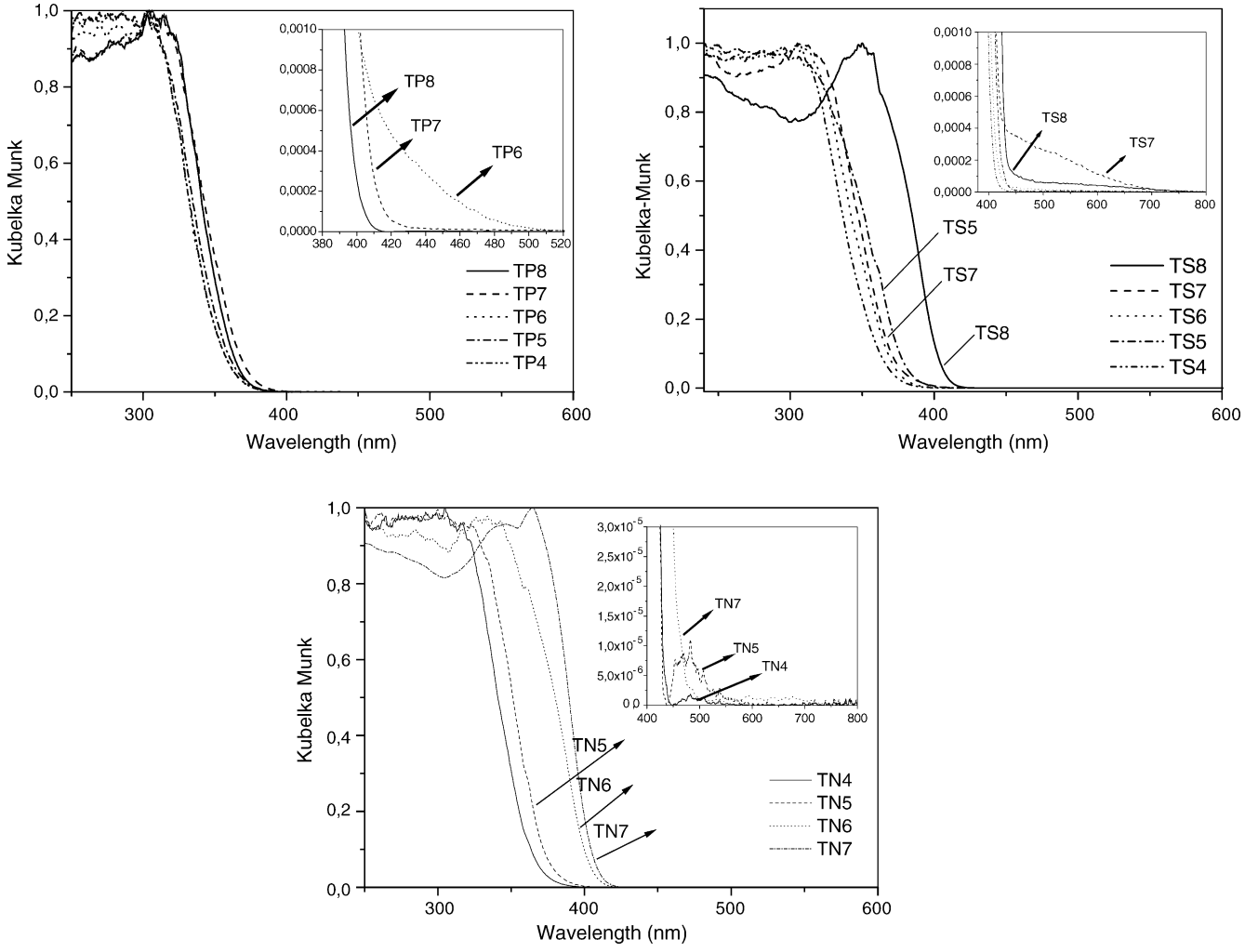

Fig. 4. Diffuse reflectance UV–vis spectra for the acid pre-treated TiO_2 catalysts calcined at different temperatures.

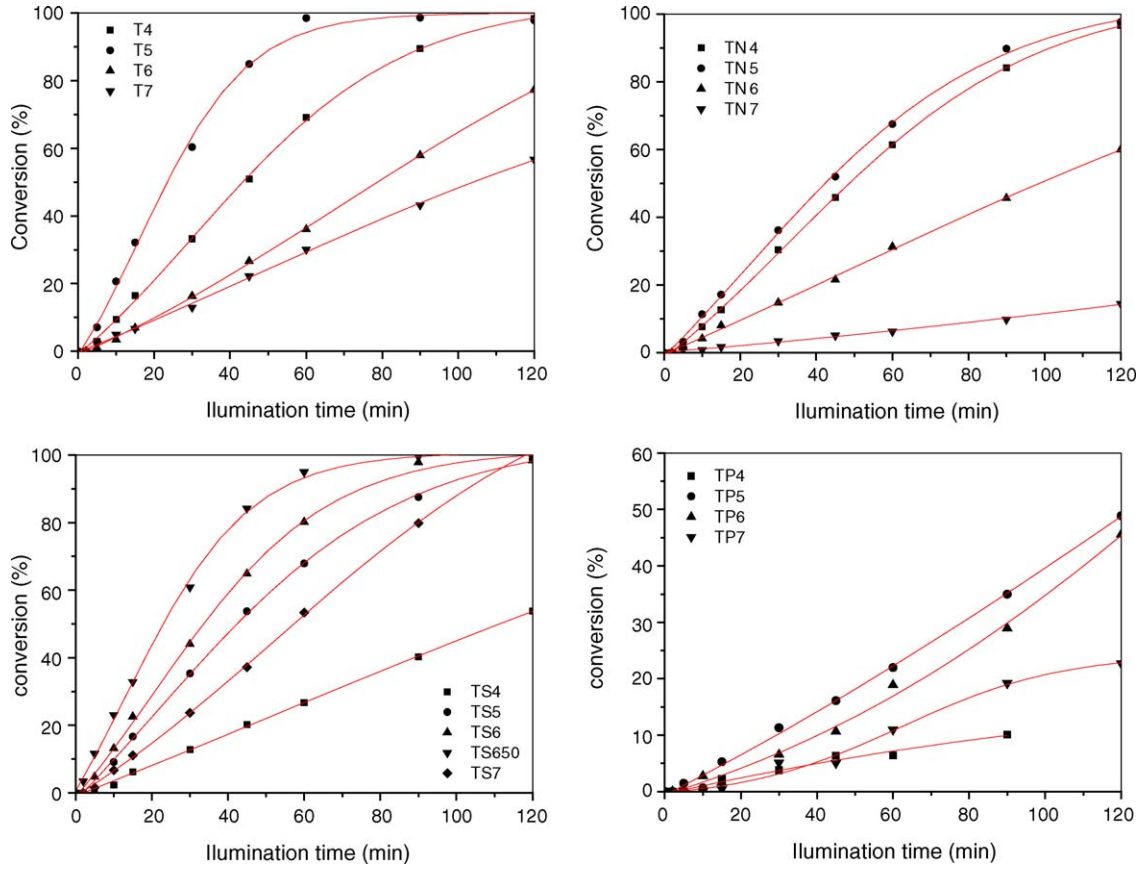

Fig. 5. Conversion plots for phenol photodegradation using the acid pre-treated TiO_2 photocatalysts calcined at different temperatures.

layer. The occurrence of "unprotected" oxygen vacancies at the surface seems to accelerate the anatase to rutile transformation. The presence of stable oxoanion is the responsible of the anatase stabilisation as well as the oxygen vacancies. These vacancies would lead to the generation of intermediate electronic states between valence and conduction band, producing the observed absorption in the visible range noticed for TS and TP system (Fig. 4).

The photocatalytic behaviour for phenol degradation over the different acid treated TiO_2 is shown in Fig. 5. As it can be noticed, untreated TiO_2 exhibits a significant decay in the conversion curve at calcination temperatures above 600 °C. Pre-treatment with nitric acid and further calcination leads to similar photocatalytic behaviour as untreated TiO_2. TS catalyst calcined at 650 °C present the best photocatalytic efficiency.

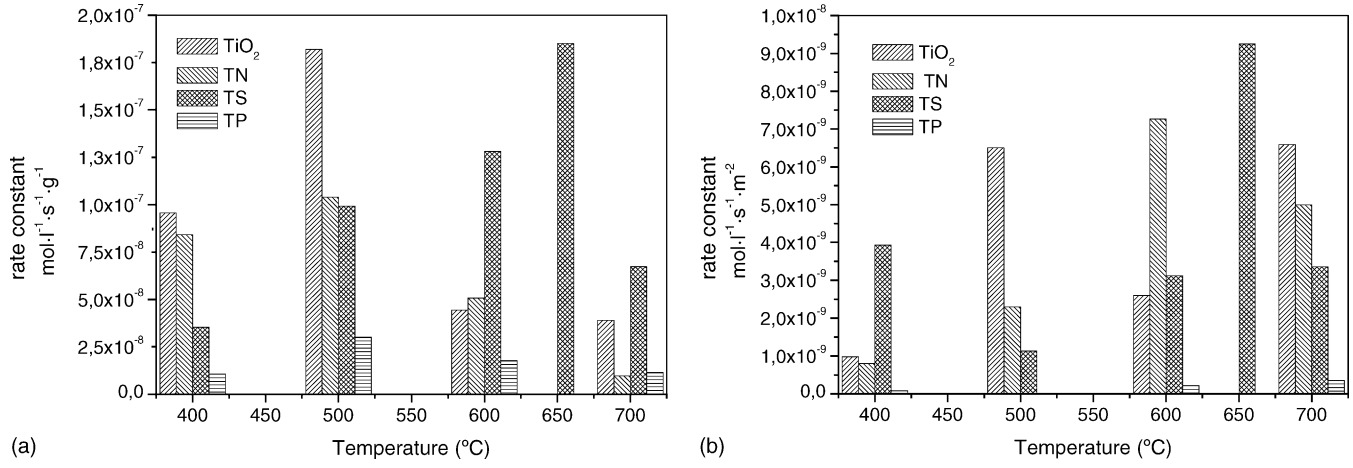

Fig. 6. Conversion rate plots for phenol photodegradation using the acid pre-treated TiO_2 photocatalysts: (a) per gram of catalyst and (b) per square metre.

Comparing the photocatalytic behaviour of this sample with the results presented above, it becomes clear that the best photocatalytic activity was achieved once the oxoanion groups have been eliminated. At this point oxygen vacancies are still stabilised at a surface position, enhancing the photocatalytic properties of the system.

Finally, TP poor photocatalytic behaviour is determined by the appearance of pyrophosphate-like species at the surface. These species are expected to appear in the surface since they come from adsorbed phosphates. Thus, it can be assumed that surface is rather covered by titanium pyrophosphates suppressing the photocatalytic activity as they formed.

Fig. 6 shows the photocatalytic reaction rate for all systems (Fig. 6a per gram and Fig. 6b per surface area of catalyst). From these plots, it is clear that the best photocatalytic behaviour corresponds to TiO_2 calcined at 500 °C and TS calcined at 650 °C. In the case of TN system, the best activity is also found for TN5 catalyst, though its conversion rate is significantly lower than that exhibited by the untreated TiO_2 calcined at the same temperature. This could indicate the detrimental effect that acid pre-treatment with nitric acid produce. Finally, TP system shows the worst photocatalytic behaviour, as expected. In order to discriminate the effect of surface area stabilisation by the acid impregnation, we have also plotted the rate constant expressed by surface area (Fig. 6b). Thus, it is clear that in the case of untreated TiO_2 the best photoactivity is limited by the higher value of the surface area together with the presence of the anatase phase. However, in the case of TS system best photocatalytic activity depends exclusively on the structural features of the catalyst determined by the presence of surface sulfates groups.

4. Discussion

On the basis of these results, acid pre-treatment of TiO_2 precursor induces important changes in the structural and morphological features of final TiO_2. The stability of each oxoanion adsorbed on TiO_2 seems to be determinant in this sense. Thus from DTG curves it is clear that nitrate is less thermal stable during calcination than sulfate and phosphate. It decomposes just at the beginning of the crystallisation process. On the contrary sulfate shows higher thermal stability, being stable up to temperatures higher than 600 °C. The extreme case would correspond to phosphate oxoanion, which is stable throughout the range of temperature studied. The stability of these oxoanions affects in a great extent to the crystallisation behaviour of TiO_2. We have reported that the surface acidification would induce the creation of oxygen vacancies during calcinations [13,19,20]. These vacancies would be stabilised at the sub-surface protected, in some way, by the presence of the oxoanion adsorbed. Once the adsorbed oxoanion evolves at different temperatures, vacancies seem to participate in the anatase to rutile transformation. It might be supposed that the aggregation of vacancies would accelerate the rutile appearance. This would be the case of nitric acid pre-treated TiO_2; adsorbed nitrate decomposed almost at the same time as the elimination of surface hydroxyl groups. Then, vacancies formation occurs at the same time as nitric decomposition, as acid OH are eliminated at the same temperature range (Figs. 1 and 4). This simultaneous process would provoke the anatase to rutile transformation. Thus, rutile appearance takes place at a lower temperature with respect to sulfate treated TiO_2 and accelerates the sintering process.

These results are in accordance with those reported by Jung et al., who described the significant role of peptisation using nitric acid at room temperature in the anatase to rutile transformation [21]. In that paper it was found that peptisation with nitric acid at room temperature leads to the formation of a rather unstable anatase structure. This unstable anatase phase obtained at room temperature would proceed, during peptisation time, towards the formation of dissolved $Ti(OH)_x$ species by a low activation energy step. After this favoured step the formation of rutile phase from $Ti(OH)_x$ intermediates would have also a low activation energy. This crystallisation pathway would be more energetically favourable than the conventional anatase to rutile transformation in a solid-state reaction. A similar mechanism in which oxygen vacancies are presents would be considered in the case of our nitric acid pre-treated TiO_2 and therefore a favoured rutilisation process takes place upon calcination.

In the case of sulfuric pre-treated TiO_2, since the thermal stability of sulfates is higher they are present at the surface till almost 700 °C. Vacancies are supposed to be formed at temperature slightly lower parallel to the bridged hydroxyl decomposition. Therefore, these oxygen vacancies become stable after the sulfate elimination. The higher stability of sulfate produces a shift in the anatase into rutile transformation toward higher temperatures. Best photocatalytic behaviour is observed for TS sample calcined at 650 °C (Fig. 6). This temperature would be the limit of the vacancies stability. Calcination at temperatures higher than 700 °C produces a rapid rutilisation process and the disappearance of vacancies. The case of phosphate is rather different. Phosphates do not present any decomposition reaction. Therefore they would represent the highest stability. However, since they remain adsorbed the whole calcination process they finally form titanium pyrophosphate species probably at the surface (Fig. 3). It is possible to observe the creation of vacancies by the emerging of a new contribution in the UV–vis spectra (Fig. 4). We could assume that in this case these vacancies would induce a new structural reorganisation and the formation of these phosphate-like species, avoiding the rutile transformation. The photocatalytic behaviour of TP samples clearly demonstrates that the surface modification proposed affects the photocatalytic process. Formation of a surface layer composed by pyrophosphate species negatively affects to the photocatalytic mechanism though anatase stabilisation is observable up to higher temperatures.

In summary, best photocatalytic behaviour for phenol degradation is achieved by a catalyst showing well-crystallised anatase phase, with relatively high surface area. It is also worthy to note that the presence of a small rutile fraction could also be of great importance [22,23]. It is expected that, during calcination, oxygen vacancies would play an important role in the structure evolution once the oxoanion is thermally decomposed. Thus, the appearance of this small rutile fraction dispersed onto the anatase matrix would be the key of the notable photocatalytic activity. Thus we could consider that TS catalyst calcined at temperature higher than 650 °C present a well crystallised anatase phase with small crystallite size (approximately 30 nm) probably mixed with a small fraction of rutile phase, generated by the occurrence of the oxygen vacancies (not detected by XRD due to the small crystallite size). On the contrary, the situation of TiO_2 calcined at 500 °C is rather different; since anatase crystallite size is significantly lower (ca. 15 nm). The synergetic effect between anatase and rutile could be explained by taking into account the Fermi levels of the two structures. This synergetic effect could be considered in two ways, as Hurum et al. [24] have been reported in the description of TiO_2 Degussa P25 photoinduced electronic processes. In one hand, if charge separation takes place in the anatase phase, part of the electrons generated by the UV-irradiation may flow into rutile phase reducing the charge recombination processes [24,25]. On the other hand, rutile could also act as antenna and therefore the charge pairs can be generated in this phase, pumping electron to lower energy anatase lattice centres leading to a more stable charge separation [24]. The charge transfer in both cases is favoured by the small crystallite size of rutile. Similar mixed system could be considered in our case, explaining the high photoactivity exhibited by TS system at such high calcination temperature.

5. Conclusions

We have performed different acid pre-treatment over TiO_2 precursor. We have previously reported the enhancement of the photocatalytic properties of pre-sulfated TiO_2. Different acids were used in this case in order to promote anatase stabilisation and oxygen vacancies formation. Results shown in the present paper confirm the mechanism of vacancy formation from an acidified surface and the role of the oxoanions in the stability of these vacancies. It is also clear the importance of the oxoanion stability in the rutilisation process and in the presence of oxygen vacancies. Best situation is observed for sulfate oxoanion since they directly control the anatase to rutile transformation and stabilise the created vacancies during calcination. Both processes are intimacy related and affect the photocatalytic efficiency of TiO_2.

Acknowledgments

Financial support by Ministerio de Ciencia y Tecnología (project ref. CTQ2004-05734-C02-02) and Junta de Andalucía (PAI group references FQM181) are acknowledged. We also like to thank NATO action (EST.CLG 979855) and Spanish–Italian action (HI02-137) for financial support.

References

[1] O.M. Alfano, D. Bahnemann, A.E. Cassano, R. Dillert, R. Goslich, Catal. Today 58 (2000) 199.
[2] D.A. Tryk, A. Fujishima, K. Honda, Electrochim. Acta 45 (2000) 2363.
[3] D.S. Bhatkhande, V.G. Pangarkar, A.A.C.M. Beenackers, J. Chem. Technol. Biotechnol. 77 (2002) 102.
[4] A. Lisenbigler, G. Lu, J. Yates, Chem. Rev. 95 (1995) 735.
[5] M.R. Hoffmann, S.T. Martin, W. Choi, D.W. Bahnemann, Chem. Rev. 95 (1995) 69.
[6] S. Yamabi, H. Imai, Chem. Mater. 14 (2002) 609.
[7] S. Yamazaki, N. Fujinaga, K. Araki, Appl. Catal. A: Gen. 210 (2004) 97.
[8] D.S. Muggli, L. Ding, Appl. Catal. B: Environ. 32 (2001) 181.
[9] W.Y. Su, X.Z. Fu, K.M. Wei, Acta Phys. Chim. Sinica 17 (2001) 28.
[10] X.Z. Fu, W.A. Zeltner, Q. Yang, M.A. Anderson, J. Catal. 168 (1997) 482.
[11] X. Deng, Y. Yue, Z. Gao, Appl. Catal. B: Environ. 39 (2002) 135.
[12] R. Gomez, T. Lopez, E. Ortis-Islas, J. Navarrete, E. Sanchez, F. Tzompanztzi, X. Bokhimi, J. Mol. Catal. A: Chem. 193 (2003) 217.
[13] G. Colón, M.C. Hidalgo, J.A. Navío, Appl. Catal. B: Environ. 45 (2003) 39.
[14] R.A. Spurr, H. Myers, Anal. Chim. 29 (1957) 760.
[15] S.K. Samantaray, K.M. Parida, J. Mater. Sci. 38 (2003) 1835.
[16] G. Munuera, A.R. González-Elipe, V. Rives-Arnau, J.A. Navío, P. Malet, J. Soria, J.C. Conesa, J. Sanz, Stud. Surf. Sci. Catal. 21 (1985) 113.
[17] O.Z. Stern, Elektrochemistry 30 (1924) 508.
[18] J.M. Criado, C. Real, J. Soria, Solid State Ionics 32–33 (1989) 461.
[19] G. Munuera, A.R. González-Elipe, V. Rives-Arnau, J.A. Navío, P. Malet, J. Soria, J.C. Conesa, J. Sanz, Stud. Surf. Sci. Catal. 21 (1985) 113.
[20] G. Colón, M.C. Hidalgo, M. Macías, J.A. Navío, Appl. Catal. A: Gen. 259 (2004) 235.
[21] H.S. Jung, H. Shin, J.R. Kim, J.Y. Kim, J.K. Lee, Langmuir 20 (2004) 11732.
[22] C. Wu, Y. Yue, X. Deng, W. Hua, Z. Gao, Catal. Today 93 (2004) 863.
[23] M. Yan, F. Chen, J. Zhang, Chem. Lett. 33 (2004) 1352.
[24] D.C. Hurum, A.G. Agrios, K.A. Gray, T. Rajh, M.C. Thurnauer, J. Phys. Chem. B 107 (2003) 4545.
[25] B. Sun, P.G. Smirniotis, Catal. Today 88 (2003) 49.